

## Responses (bule) to Reviewer's comments (black)

This paper uses a mass balance approach to interpret observations of TROPOMI NO<sub>2</sub> columns and CEMS NO<sub>x</sub> emission flux, enabling the propagation of measured flux at in situ sites to build seamless monthly NO<sub>x</sub> emission estimates across Shanxi Province, China. It also further interprets the variability of derived model parameters in their framework that represent NO<sub>x</sub>/NO<sub>2</sub> emission ratio ( $\alpha_1$ ), NO<sub>x</sub> lifetime ( $\alpha_2$ ) and horizontal advection rate ( $\alpha_3$ ). To my knowledge, this is a pioneering study that evaluates and interprets an established space-borne emission estimation method, which has rarely been validated using densely distributed flux observations. The paper is overall well-written with sound methods and results. At the same time, some critical details are missing, and structural changes of the contents are needed. I support the publication of this manuscript, provided that the following comments can be addressed.

Major comments:

1) The MFIEF approach is largely originated from similar box-modeling ideas in previous studies (Beirle et al., 10.1126/sciadv.aax98, 2019; Kong et al., 10.5194/acp-19-12835-2019, 2019), while differs to some extent in details about assumptions on each source/sink process. Line 84-86 presents these studies in the overall "previous study" category, which seem to diminish this connection. I suggest the authors to introduce these approaches in the end of this paragraph, and acknowledge the similarity of idea used in this paper. Also, certain discussions about the uniqueness and capabilities of MFIEF (e.g., using measured emissions, fitting variable parameters that were fixed in previous approaches, etc.) relative to these previous methods should also be added in the Introduction and/or Discussion Section.

We have reorganized the final paragraphs of the Introduction in the following way.

“This approach is partly originated from similar box-modeling ideas in previous studies (Rigby et al., 2008; Beirle et al., 2019; Kong et al., 2019), which themselves are based on previous theory underlying the development of mass-conserving box models (Seigneur et al., 1986). In this specific work, the mass of emissions is connected with the in-situ observed column loadings through application of the following factors: the

temporal rate of change in column loading, first order chemical loss of  $\text{NO}_x$ , gradient transport of  $\text{NO}_x$ , and gradient transport of atmospheric airmass. The coefficients weighting these terms are flexibly fitted, allowing a wider range of possible driving forces and solutions to be considered, while still requiring that these parameters are consistent with observations (Rollins et al., 2012; Karl et al., 2023). The fitted relationship is formed without the use of complex models, can be run on a normal desktop computer, and the end product can be flexibly modified by the user for their own various applications”.

The content of other relevant parts has also been changed.

2) The UVAI is used as a proxy of OH and  $\text{NO}_x$  lifetime to interpret EOF2. However, UVAI is a measure of aerosol absorption, while the actual radiation flux reach surface is also sensitive to aerosol scattering, cloud extinction, and solar angles. I did not find existing literature reporting strong correlation between UVAI and OH or  $\text{NO}_x$  lifetime, so it is not convincing for me to justify the interpretation related with Figure 11. Please provide stronger evidence to justify the use of UVAI, or switch to use other parameters (e.g.,  $\alpha_2$ ?).

We agree that satellite observations of the ultraviolet aerosol index (UVAI) are a measure of aerosol absorption. The absorbing aerosols inferred from the UVAI in turn absorb, scatter, and extinct radiation across all wave bands in the visible and UV portions of the spectrum. This in turn directly impacts all wavebands involved with atmospheric chemistry and climate radiative forcing. This has been demonstrated in numerous studies reporting that absorbing aerosols affect the downwelling surface radiative forcing in the visible (and therefore the actinic flux) (Léon, 2002) as well as OH concentrations (Hammer et al., 2016). Therefore, UVAI indirectly is one component of the chemical decay capacity of  $\text{NO}_x$  in-situ. Since it is observed on the same platform as the  $\text{NO}_2$  observations and the reasons provided above, it is introduced here for comparison with EOF2. The fact that they are correlated during peak event times provides strong evidence that during these peak times, the chemical decay of  $\text{NO}_x$  is strongly related to the in-situ absorbing aerosol column loading.

3) Section 3.3: besides introducing the total uncertainties, contributions from each factor should also be included. One particularly important source is the performance of the fitting and the consequent errors in each parameter. This is the most fundamental information to evaluate the fidelity of the MFIEF framework. How much variability of observed  $VNO_2$  and  $ENO_x$  can be explained by Eq. (3)? As the fitting is performed including all observations, is it unbiased for all months and grids?

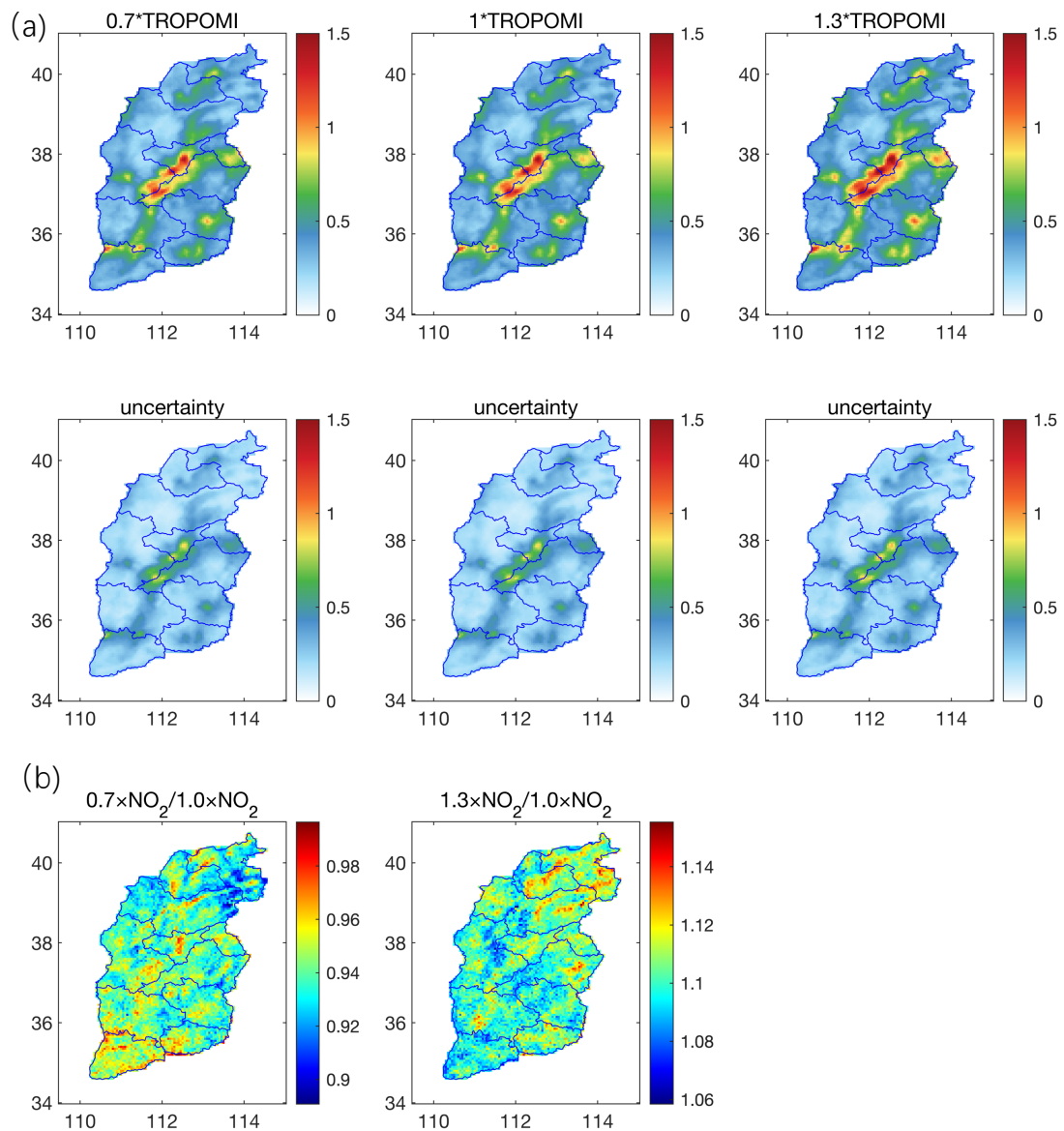
In addition to introducing the total uncertainties, a sensitivity test has been performed to test the robustness of the fits. This is done by making the assumption that the TROPOMI  $NO_2$  column values are actually observed near the extreme top and bottom of their  $\pm 30\%$  uncertainty range. When the TROPOMI  $NO_2$  column values are changed, all factors are simultaneously changed. This set of uncertainty runs is applied uniformly as two separate cases: 70% case (in which the  $NO_2$  columns are multiplied by 0.7) and 130% case (in which the  $NO_2$  columns are multiplied by 1.3). The coefficients were refit using these new values from TROPOMI and the same values from both CEMS and meteorology over the entire domain included in this work. The results are provided in Response Figure 1.

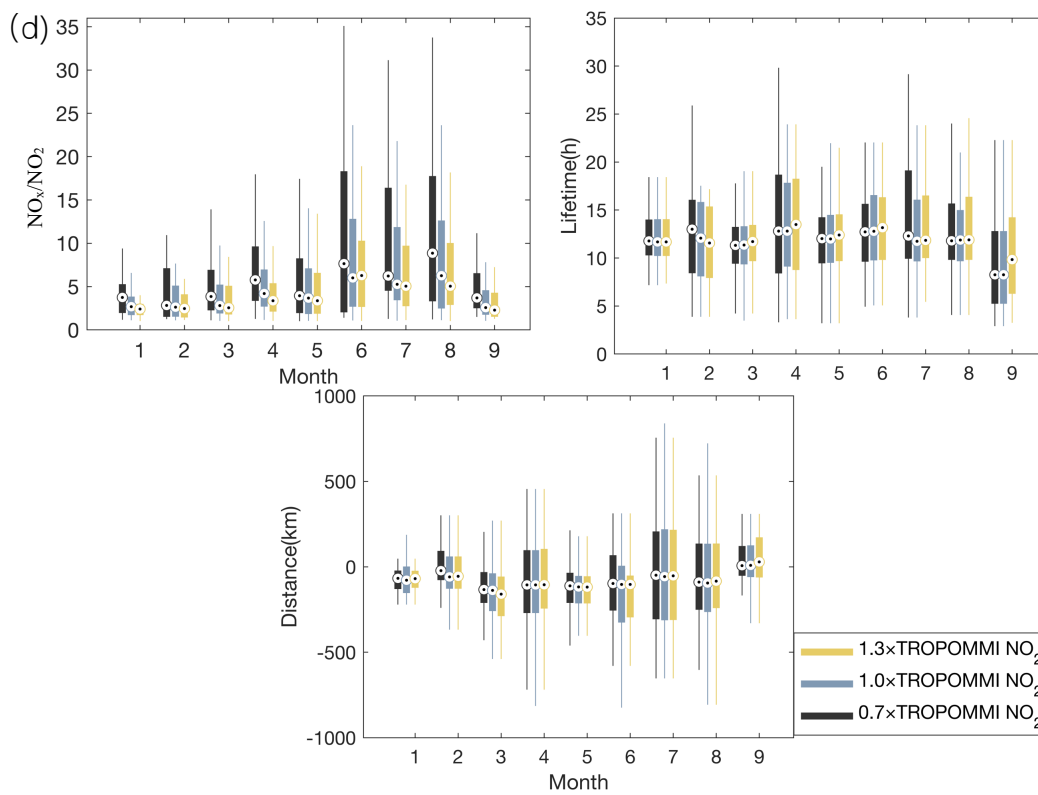
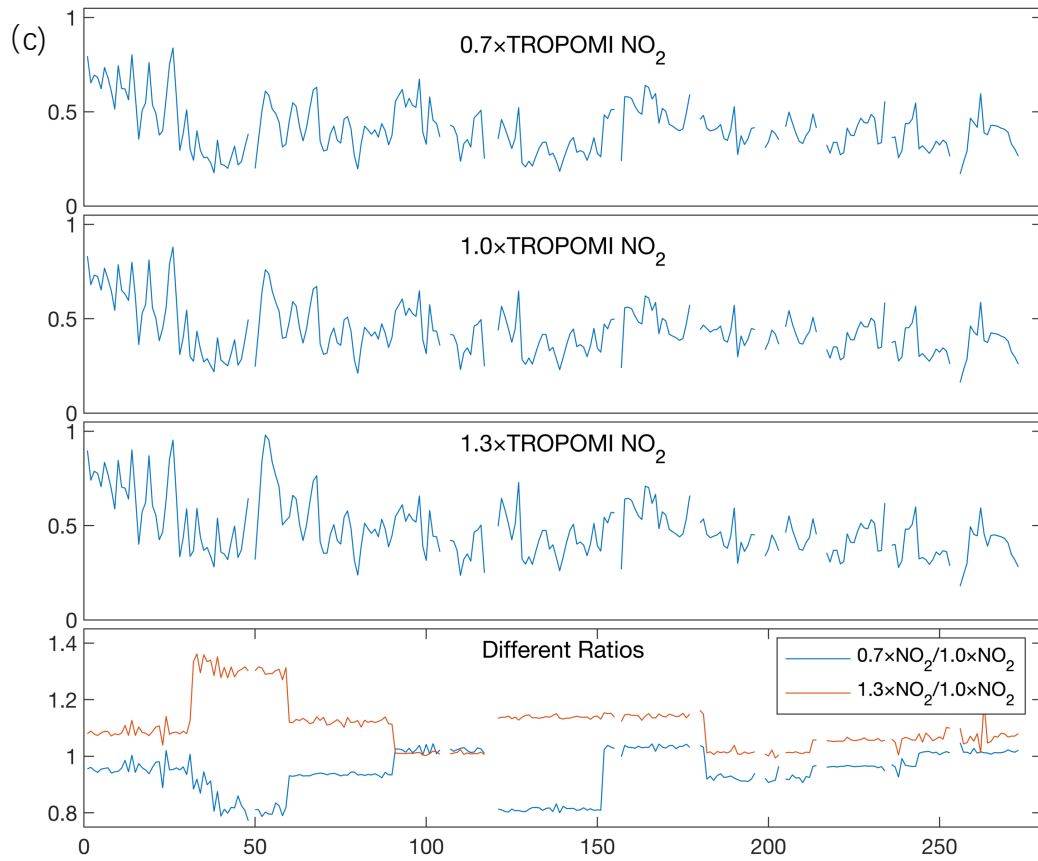
First, it is observed that in terms of the spatial map and temporal change, that the new  $NO_x$  emissions in the 70% case are always larger than 0.7 times the original emissions case (spatially annually averaged and grid-by-grid this varies from 0.89 to 1.00, while temporally domain averaged this varies from 0.77 to 1.04). Similarly, the new  $NO_x$  emissions in the 130% case over the median 90% of data is smaller than 1.3 times the original emissions case (spatially annually averaged and grid-by-grid this varies from 1.08 to 1.12 while temporally domain averaged this varies from 1.01 to 1.30).

Second, the constraints on the physically realistic values of  $\alpha_1$  and  $\alpha_2$ , as well as the constant use of CEMS provide a negative feedback loop on the relationship between the  $NO_2$  column changes and the final emissions products. This is consistent with the observed computed emissions and differences.

Third, the best fit values of  $\alpha_1$ ,  $\alpha_2$ , and  $\alpha_3$  in each case 70%, 100%, and 130% on a month-by-month basis are always found within the central 50% of the distribution of

each other. Furthermore, while the breadth of the different values does change slightly, in some months, it is always either increasing or decreasing on both edges, not only in one direction. These findings indicate that any changes in the parameters between the different NO<sub>2</sub> column loading cases are generally smooth, consistent, provide redundancy to each other, and are also influenced significantly by the a priori emissions used in the fitting.





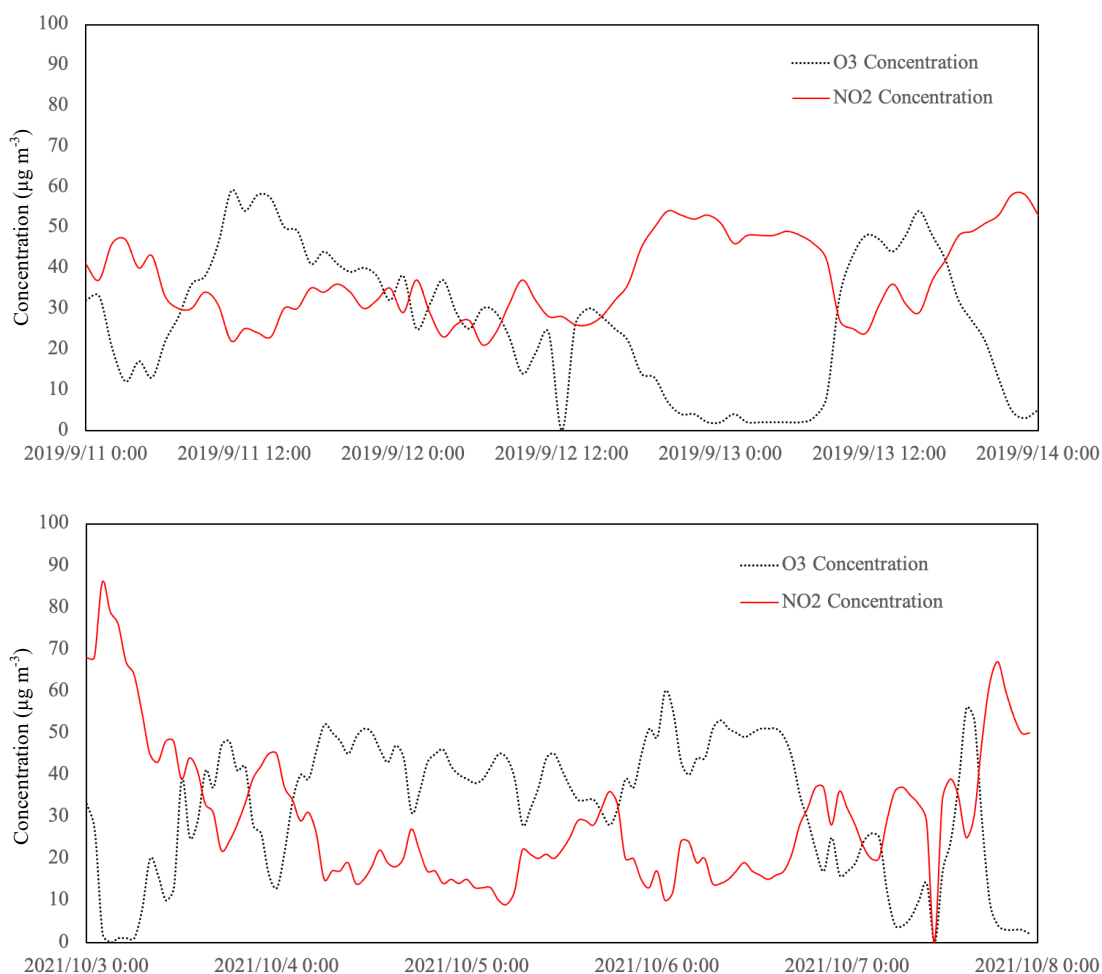
**Response Figure 1.** Different TROPOMI NO<sub>2</sub> for emission calculation based on CEMS using MFIEF: (a) 70%, 100%, 130% cases calculated emission and their uncertainty; (b) the differences between 70% to 100% case and 130% to 100% case; (c) time series of 70%, 100%, 130% cases and their differences; (d)  $\alpha_1$ ,  $\alpha_2$ , and  $\alpha_3$  in each case.

4) Section 3.4: The derived emissions are representative of ambient fluxes (instead of initial emissions from the furnace), so the rapid NO-NO<sub>2</sub> conversion and consequently the NO<sub>x</sub>/NO<sub>2</sub> ratio is dependent on not only the combustion environment factors discussed in the manuscript, but also ambient chemistry (e.g., photolysis rate and ozone concentration). I assume the latter factor might be more important in driving the seasonal variations in Figs. 12 and 14. Due to the lack of full consideration of all driving factors as well as the lack of outstanding hotspot of alpha1 from certain month or factory, the current discussion of alpha1 in this section is relatively more conjectural than the other part of the paper. My overall suggestion is to greatly reduce the amount of discussion and focus on 1-2 most convincing observations that can be concluded from existing data, with acknowledgement of various factors driving alpha1 variability and precluding a full explanation of all revealed variabilities.

Initially, the ratio of  $\alpha_1$  is entirely determined at the source as a function of the type of source, its thermodynamic conditions, availability of nitrogen and oxygen, water vapor, etc. However, after emissions into the atmosphere there is a rapid adjustment that occurs from the extremely hot air emitted at the stack or pipe exit until it comes to equilibrium in terms of both vertical height and thermodynamic condition. During this period of time, further modification occurs.

However, the assertion that such chemistry or thermodynamic changes are important is based on many assumptions, which themselves are not necessarily valid in the real atmosphere.

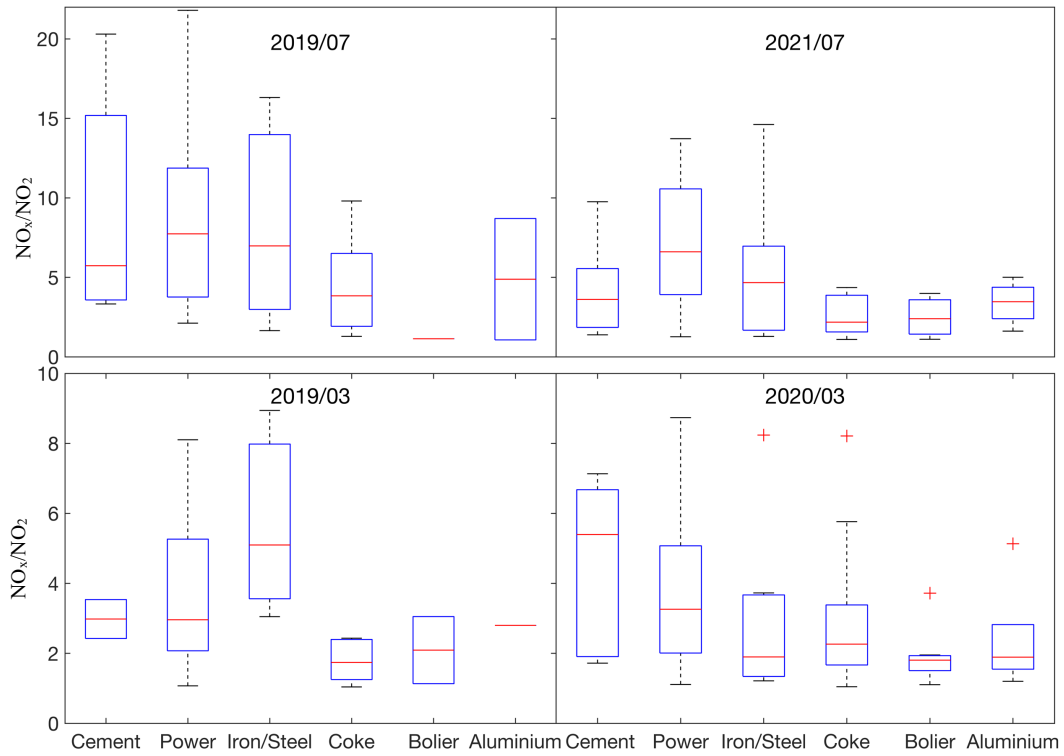
1. There are many observations in this area that demonstrate at times there is insufficient ozone present at the surface to convert NO<sub>2</sub> to NO even on days which have a high surface temperature, which should be the times with the largest surface O<sub>3</sub> concentration (Response Figure 2).
2. The column ozone is even lower than the surface ozone, so the fraction of the emissions which buoyantly break into the free troposphere or are lofted by upslope winds will always encounter ozone which is too low to lead to chemical titration.



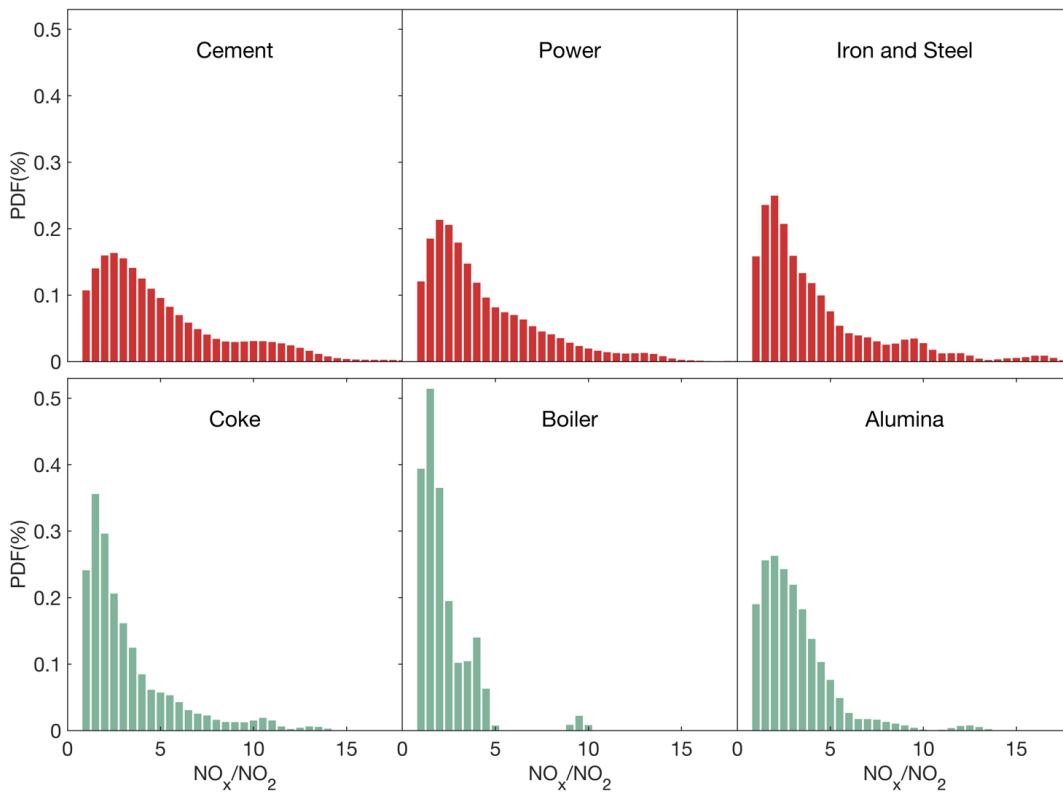
**Response Figure 2.** Time series of hourly concentration of O<sub>3</sub> and NO<sub>2</sub> from ambient air quality monitoring stations near an iron and steel factory in Taiyuan City.

Furthermore, while there is modification observed from different months of the year on the mean and standard deviation of the value of  $\alpha_1$ , that the types with larger  $\alpha_1$  are still larger and the types with smaller  $\alpha_1$  are still smaller (Response Figure 3). This indicates that indeed the original thermodynamics still plays an important role in determining the value of  $\alpha_1$ .

Since the climatology across the regions which have these sites is roughly similar, the only things over the 3-years of data that can distinguish these sites from each other are the source type of emissions and the TROPOMI NO<sub>2</sub> column loading (Response Figure 4).



**Response Figure 3.** Distribution of  $\alpha_1$  during certain warm and cold month at cement factories, power plants, steel and iron factories, coke ovens, boilers, and aluminium oxide factories.



**Response Figure 4.** Histogram of  $\alpha_1$  calculated based on CEMS using MFIEF at cement factories, power plants, steel and iron factories, coke ovens, boilers, and aluminum oxide factories.



Specific comments:

1) Line 22-23: As outlined before, the statement of "significant correlation with combustion temperature and energy efficiency" might be too strong here.

We have slightly toned down the strength of this statement.

2) Line 39: delete "are more serious".

We agree and have removed this phrase.

3) Line 48: delete "(2015, 2020)".

The reference format has been modified.

4) Citations in the Introduction Section:

Line 42: should also cite Zhang et al., 10.1073/pnas.1907956116, 2020; Wang et al., 10.1073/pnas.2007513117, 2020; Li et al., 10.1016/j.scitotenv.2021.150011, 2022; Wei et al., 10.5194/acp-23-1511-2023, 2023.

These (and other) references have been added to the revised version. Thank you for pointing out these interesting scientific works.

Line 54: (Beirle et al., 2011) is not a paper studying NO<sub>x</sub> forming aerosol.

We agree. We believe that Rollins et al. (2012) is a better fit here. This has been updated.

Line 56: Besides China, some other regional inventories (e.g., McDonald et al., 10.1021/es401034z, 2013; Xing et al., 10.5194/acp-13-7531-2013, 2013) might be worth citing.

These (and other) references have been added to the revised version. Thank you for pointing out these interesting scientific works.

Line 92: can cite (Zheng et al., 10.5194/acp-18-14095-2018, 2018) for MEIC.

This line has been moved to the methods and the reference has been appropriately updated.

5) Line 85-86: As outlined before, should clarify that your approach improves these assumptions to some extent.

We have deleted this sentence, and further reorganized the entire final paragraph of the Introduction. It now reads:

“This approach is partly originated from similar box-modeling ideas in previous studies (Rigby et al., 2008; Beirle et al., 2019; Kong et al., 2019), which themselves are based on previous theory underlying the development of mass-conserving box models (Seigneur et al., 1986). In this specific work, the mass of emissions is connected with the in-situ observed column loadings through application of the following factors: the temporal rate of change in column loading, first order chemical loss of NO<sub>x</sub>, gradient transport of NO<sub>x</sub>, and gradient transport of atmospheric airmass. The coefficients weighting these terms are flexibly fitted, allowing a wider range of possible driving forces and solutions to be considered, while still requiring that these parameters are consistent with observations (Rollins et al., 2012; Karl et al., 2023). The fitted relationship is formed without the use of complex models, can be run on a normal desktop computer, and the end product can be flexibly modified by the user for their own various applications.” Showing some extent of us on the box-modeling and mass balance idea.

6) Line 91-92: These two are bottom-up inventories, so should follow after Line 73? I do not see clear connection of this sentence with the previous text.

This sentence has been modified and moved to the Materials and Methods section.

7) Line 98: What idea from bottom-up inventory is used in your approach?

The MFIEF approach uses an emissions inventory as the a priori to begin the inversion. This work uses two different emissions inventories: one is bottom-up derived from observed CEMS fluxes, while the other is fully bottom up MEIC.

8) Line 107: As outlined before, using UVAI as a proxy of UV radiation seems not appropriate.

As we have responded above, UVAI is a measurement that provides information on the column loading of absorbing aerosol in the UV. This absorbing aerosol in turn impacts the radiative flux at all visible and UV bands through absorption, scattering, and extinction. There has been extensive work which has demonstrated that the absorbing aerosols reduce the actinic flux and alter OH. In both cases, this has an impact on the atmospheric lifetime of NO<sub>x</sub>. We agree that this is not the only component, but we do believe that it is fair to say that UVAI has an impact on the net actinic flux at the surface.

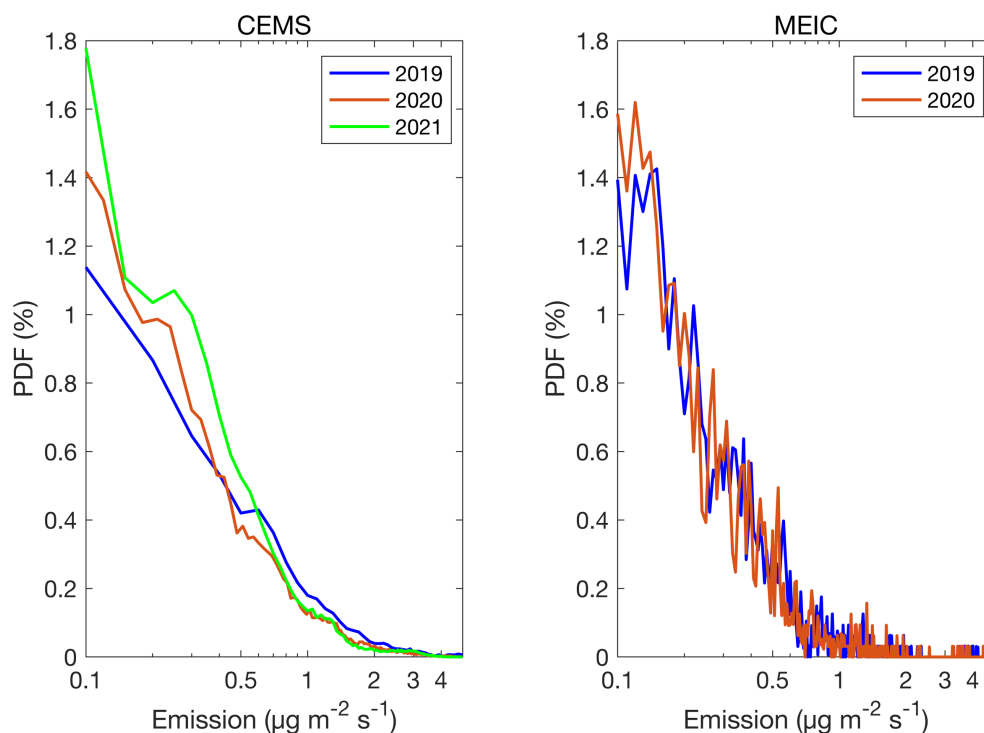
We have modified the paper as: “different actinic flux and atmospheric oxidation”

9) Fig. 3c and 4c: set log-scale for x-axis might increase the readability of the figure. Also, 28% of days are absent in 2019 so would that affect the sampling and representativeness of data in Fig. 3?

The x-axis has been changed into log-scale (Response Figure 5).

Since there is insufficient CEMS data for November and December 2019 to fit the equations, the results of the month-by-month calculations of emissions during those two months is reflective of the fitted values of  $\alpha_1$ ,  $\alpha_2$ , and  $\alpha_3$  from other similar conditions, which includes data from November and December in other years, as well as surrounding data from January and February. These are conditions in which there should be somewhat similar climatological factors such as temperature, actinic flux, wind, and other environmental data which impacts upon the observed NO<sub>2</sub> column from TROPOMI. At all times, the actual TROPOMI NO<sub>2</sub> column observations are used to constrain its emissions field. This is consistent with the production methods of

the companies and the requirements for production stoppages and restrictions in general.



**Response Figure 5.** PDFs of day-by-day and grid-by-grid emissions of CEMS and MEIC over individual years (with log-scale for x-axis).

The CEMS data from 2018 through the present indicates that the missing times in 2019 are found near the median range of the distribution, and therefore are not biased.

10) Line 211: this is true for daytime and locations with strong  $\text{NO}_x$  emissions only. See (Kenagy et al., 10.1029/2018JD028736, 2018) for nighttime sinks, and (Romer Present et al., 10.5194/acp-20-267-2020, 2020) for possible significant daytime sink via reactions with  $\text{RO}_2$ . As Eq. 3 relates  $\text{VNO}_2$  at afternoon overpass to 24-h mean emissions, the lifetime should also reflect all hours during the day.

We agree that this work is reflective of the different chemical loss sources which occur throughout the day, and also throughout the column where the emissions spread to. This must therefore include actinic flux derived chemical reactions (i.e.,  $\text{RO}_2$  during the daytime), heterogeneous surfaces (i.e.,  $\text{N}_2\text{O}_5$ ), and other reactions which

happen in the free troposphere under much colder and lower pressure conditions as a considerable amount of the flux is rapidly brought up to elevation by upslope winds in this region. The net linear coefficient  $\alpha_2$  is a reflection of the net total 24-hour, atmospheric column chemical first order loss coefficient. This is a very interesting area for further study to see if and how simple non-linearity could be brought into better constraining the chemical loss term for future applications of this work.

The following changes have been made: “The second of these is the chemical loss of  $\text{NO}_x$ , which will always lead to a decrease in the stock. The chemical sink of  $\text{NO}_x$  is dominated by the reaction between  $\text{NO}_2$  and OH, via reactions with products formed from the actinic flux (i.e., chemistry such as  $\text{RO}_2$ ), and on aerosol surfaces via heterogeneous reactions (Valin et al., 2013; Kenagy et al., 2018; Romer Present et al., 2020), which herein is described as S”.

11) Equation 3: Since  $V_{\text{NO}_2}$  is a snapshot of afternoon overpass while  $E_{\text{NO}_x}$  is 24-h average, so  $\alpha_1$ - $\alpha_3$  all contain the conversion from overpass time to 24-h mean. Should acknowledge this fact.

This part is now explained in greater detail, including the fact that TROPOMI has some days with a single overpass, and other days with two separate overpasses approximately 101.5 minutes apart at the same location. During this specific subset of days, information from both overpasses is used on average.

“ $V_{\text{NO}_2}$  is observed as either one or two overlapping snapshots of total column information occurring at 13:30 LT (and under some conditions also 101.5 minutes either earlier or later (Tonion and Pirotti, 2022)). In all cases, the meteorological values and CEMS values are representative of 24-hour total and/or daily average conditions respectively. Therefore, the fitted values of  $\alpha_1$ ,  $\alpha_2$ , and  $\alpha_3$ , as presented are representative of 24-hour average or 24-hour net effect respectively, acting on the entire column of  $\text{NO}_x$ ”.

12) Fig. 5: As outlined before,  $\alpha_1$  is not just determined by type of source.

$\alpha_1$  is determined in significant part by the type of source, its thermodynamic conditions, and availability of nitrogen and oxygen. This is also modified based on rapid chemistry or thermodynamics which occur in the in-situ atmosphere. However, there are many observations in this area which demonstrate that at times there is insufficient ozone present to convert  $\text{NO}_2$  to  $\text{NO}$ , indicating that in many cases, the rapid atmospheric adjustment is not actually happening. Furthermore, the emissions include not only what ends up in boundary layer, but also the fraction above the boundary layer, which occurs through upslope winds and plume rise. The chemistry above the boundary layer tends to be far slower and the controlling factors frequently are different in nature. The effects of the change also are averaged over 24 hours, and therefore include night-time as well as day-time types of effects, as previously mentioned.

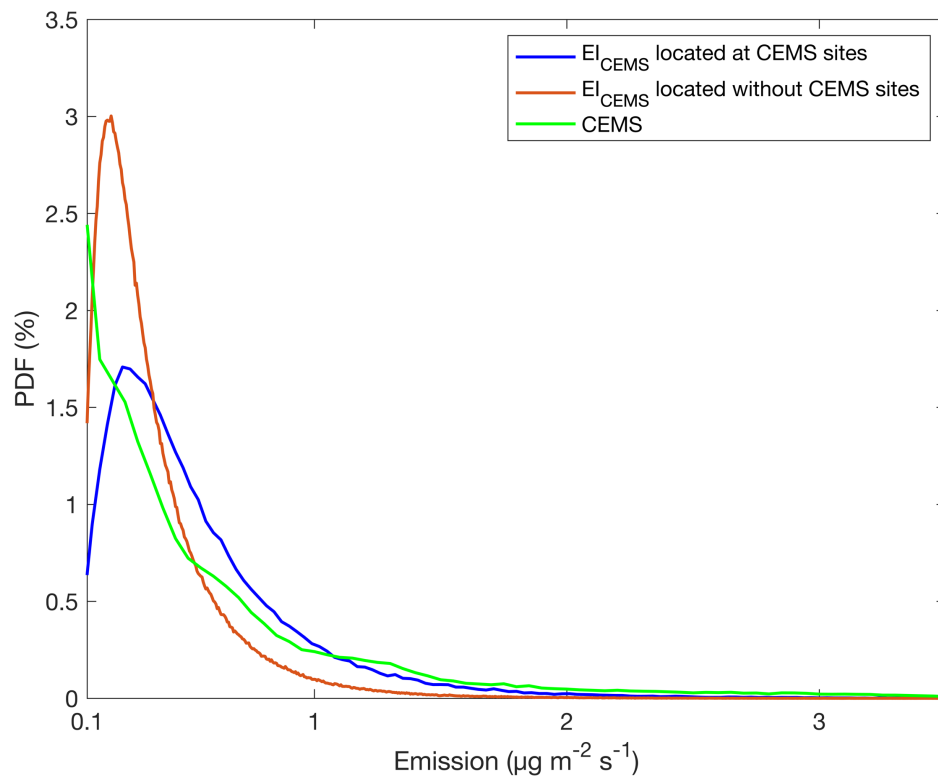
13) Fig. 6: a scatter plot of Fig. 6a vs. Fig. 3a will provide an insight about how representative Eq. 3 is. Certain locations with strong emissions while unmeasured by Fig. 3a should also be discussed (e.g., are these exactly locations of missed stationary sources?).

PDFs of the a priori emissions (CEMS, Fig. 3a),  $\text{EI}_{\text{CEMS}}$  (Fig. 6a) at locations which have CEMS data, and  $\text{EI}_{\text{CEMS}}$  at locations which do not have CEMS data, are calculated PDFs using all data on a day-by-day and grid-by-grid basis in Response Figure 6. As demonstrated, the value of emissions computed at CEMS sites is slightly larger in the mean and median than the values of emissions computed off CEMS sites, in particular between emissions in the range from  $0.5$  to  $1.5 \mu\text{g m}^{-2} \text{s}^{-1}$ . However, at the extremes even the  $\text{EI}_{\text{CEMS}}$  locations without CEMS data has both high and very low values. This is due to the fact that CEMS sites do not include traffic, residential, and small industrial sources. Therefore, there are some net high emissions sources in some regions that have no CEMS data available.

These results demonstrate that this approach is sufficiently flexible that it can be applied to identify and roughly estimate emissions from areas in which the conditions are similar to but not absolutely the same as those at which the training occurs. We have demonstrated that there is enough data from the existing CEMS network to train the

model to reproduce emissions over the entire range of values observed in Shanxi. This is due to the fact that the training has occurred over a sufficiently wide range of input conditions, TROPOMI NO<sub>2</sub> columns, meteorology, and other forcing factors.

The comparison with the actual CEMS data shows that both emissions datasets are more central than the CEMS data. This also makes sense, since there is no grid in which 100% of the total sources are due to only CEMS. It also is factually true that in the real atmosphere, the actions of transport and diffusion will tend to reduce very large values and fill in very small values.



**Response Figure 6.** The distribution of EI<sub>CEMS</sub> with and without CEMS data, and CEMS.

14) Fig. 8: What spatial extent is used to calculate the city-mean emissions? If the range is too small, the difference between MEIC and CEMS could be dominated by dilution by the large grid cell.

First, our resolution is 0.05°×0.05°, which is higher than the 0.25°×0.25° MEIC product used. However, the number of grids per city is far more than the offset ratio of 25. The

number of grids in each city is show on the table below. We think that the grids number is enough to calculate the difference between MEIC and CEMS.

**Response Table 1.** The number of grids in each city

City	TY	DT	YQ	CZ	JC	SZ	JZ	YC	XZ	LF	LL
No. of grids	289	591	183	566	375	446	663	565	1045	818	866

15) Fig. 9: Are the spatial distribution of EOF1 correlating with that of alpha1? How about EOF2 vs. alpha2? EOF3 vs. divergence?

Spatial correlation was performed grid-by-grid between the three-year average of  $\alpha_1$  and EOF1, where  $r=0.18$ ,  $p<0.01$ , indicating that there is a statistically significant correlation, but one which is far less significant than the result currently presented.

Similarly, correlation was performed grid-by-grid between three-year average of  $\alpha_2$  and EOF2, where  $r=0.15$ ,  $p=0.012$ , indicating that there is also a statistically significant correlation, but one which is far less significant than the result already presented. The correlation between EOF3 and divergence is already displayed in the paper (fig.12).

16) Sections 3.1 and 3.2: Alpha1-alpha3 all exhibit certain spatial and temporal variabilities. What are the implications on previous methods that have simpler (e.g., fixed) assumptions?

In Beirle et al. (2019)  $\alpha_1=1.32 \pm 0.26$  and  $\alpha_2=4 \pm 1.3$  hours. These results determine that 19% of total sites have as value of  $\alpha_1$  inside of their range of fixed  $\alpha_1$ , while 79% of sites have a value of  $\alpha_1$  larger and 2% of sites have a value of  $\alpha_1$  smaller than allowed by previous approaches. Furthermore, only 4% of the total sites in this work have as value of  $\alpha_2$  inside their range of fixed  $\alpha_2$  and 96% of sites have a value of  $\alpha_2$  larger than allowed by previous fixed assumption approaches. For these reasons, using the fixed assumptions approach would lead to a large majority of the grids in this work having an emissions value which is not properly predicted. The magnitude of emissions is also biased based on their range, in particular with Power Plants/Steel Factories/Cement factories having values of  $\alpha_1$  and  $\alpha_2$  which are far outside of the



ranges of their fixed studies, while also being grids with higher absolute emissions values.

17) Line 462: should mention possible benefits from Geostationary instruments that can be promising to resolve the expectedly strong diurnal variability of  $\alpha_1$ - $\alpha_3$ .

This is an excellent suggestion. The following change has been made to the text:

This work would be improved by reduction in remotely sensed measurement errors/uncertainties, increased use of and access to surface CEMS and other high quality surface flux measurements, improved a priori emissions databases, and higher frequency temporal data availability from new geostationary satellite platforms.

## References

- Beirle, S., Borger, C., Dorner, S., Li, A., Hu, Z. K., Liu, F., Wang, Y., and Wagner, T.: Pinpointing nitrogen oxide emissions from space, *Sci. Adv.*, 5, <https://doi.org/10.1126/sciadv.aax9800>, 2019.
- Hammer, M. S., Martin, R. V., van Donkelaar, A., Buchard, V., Torres, O., Ridley, D. A., and Spurr, R. J. D.: Interpreting the ultraviolet aerosol index observed with the OMI satellite instrument to understand absorption by organic aerosols: implications for atmospheric oxidation and direct radiative effects, *Atmos. Chem. Phys.*, 16, 2507-2523, <https://doi.org/10.5194/acp-16-2507-2016>, 2016.
- Karl, T., Lamprecht, C., Graus, M., Cede, A., Tiefengraber, M., Vila-Guerau de Arellano, J., Gurarie, D., and Lenschow, D.: High urban  $\text{NO}_x$  triggers a substantial chemical downward flux of ozone, *Sci. Adv.*, 9, eadd2365, <https://doi.org/doi:10.1126/sciadv.add2365>, 2023.
- Kenagy, H. S., Sparks, T. L., Ebben, C. J., Wooldrige, P. J., Lopez-Hilfiker, F. D., Lee, B. H., Thornton, J. A., McDuffie, E. E., Fibiger, D. L., Brown, S. S., Montzka, D. D., Weinheimer, A. J., Schroder, J. C., Campuzano - Jost, P., Day, D. A., Jimenez, J. L., Dibb, J. E., Campos, T., Shah, V., Jaeglé, L., and Cohen, R. C.:  $\text{NO}_x$  lifetime and  $\text{NO}_y$  partitioning during winter, *J. Geophys. Res. Atmos.*, 123, 9813-9827, <https://doi.org/10.1029/2018jd028736>, 2018.
- Kong, H., Lin, J., Zhang, R., Liu, M., Weng, H., Ni, R., Chen, L., Wang, J., Yan, Y., and Zhang, Q.: High-resolution ( $0.05^\circ \times 0.05^\circ$ )  $\text{NO}_x$  emissions in the Yangtze River Delta inferred from

- OMI, *Atmos. Chem. Phys.*, 19, 12835-12856, <https://doi.org/10.5194/acp-19-12835-2019>, 2019.
- Léon, J. F.: Aerosol direct radiative impact over the INDOEX area based on passive and active remote sensing, *J. Geophys. Res.*, 107, <https://doi.org/10.1029/2000jd000116>, 2002.
- Rigby, M., Prinn, R. G., Fraser, P. J., Simmonds, P. G., Langenfelds, R. L., Huang, J., Cunnold, D. M., Steele, L. P., Krummel, P. B., Weiss, R. F., O'Doherty, S., Salameh, P. K., Wang, H. J., Harth, C. M., Mühle, J., and Porter, L. W.: Renewed growth of atmospheric methane, *Geophys. Res. Lett.*, 35, <https://doi.org/10.1029/2008gl036037>, 2008.
- Rollins, A. W., Browne, E. C., Min, K. E., Pusede, S. E., Wooldridge, P. J., Gentner, D. R., Goldstein, A. H., Liu, S., Day, D. A., Russell, L. M., and Cohen, R. C.: Evidence for NO<sub>x</sub> Control over Nighttime SOA Formation, *Science*, 337, 1210-1212, <https://doi.org/10.1126/science.1221520>, 2012.
- Romer Present, P. S., Zare, A., and Cohen, R. C.: The changing role of organic nitrates in the removal and transport of NO<sub>x</sub>, *Atmos. Chem. Phys.*, 20, 267-279, <https://doi.org/10.5194/acp-20-267-2020>, 2020.
- Seigneur, C., A. B. Hudischewskyj, J. H. Seinfeld, K. T. Whitby, E. R. Whitby, J. R. Brock, and H. M. Barnes, Simulation of aerosol dynamics: A comparative review of mathematical models, *Aerosol Sci. Technol.*, 5, 205-222, <https://doi.org/10.1080/02786828608959088>, 1986.
- Tonion, F. and Pirotti, F.: Sentinel-5p NO<sub>2</sub> data: cross-validation and comparison with ground measurements, ISPRS Archives, XLIII-B3-2022, 749-756, <https://doi.org/10.5194/isprs-archives-XLIII-B3-2022-749-2022>, 2022.
- Valin, L. C., Russell, A. R., and Cohen, R. C.: Variations of OH radical in an urban plume inferred from NO<sub>2</sub> column measurements, *Geophys. Res. Lett.*, 40, 1856-1860, <https://doi.org/10.1002/grl.50267>, 2013.